Available online at www.sciencedirect.com

ScienceDirect

Solar Energy 96 (2013) 253–262

SOLAR ENERGY

www.elsevier.com/locate/solener

Electrical performance analysis of PV modules with bifacial silicon solar cells and white diffuse reflector

A. Moehlecke, F.S. Febras, I. Zanesco *,[1]

Solar Energy Technology Nucleus – NT-Solar, Faculty of Physics, Pontifical Catholic University of Rio Grande do Sul, PUCRS, Av. Ipiranga, 6681, Prédio 96A, Porto Alegre, RS CEP 90619-900, Brazil

Received 27 March 2013; received in revised form 15 June 2013; accepted 22 July 2013
Available online 15 August 2013

Communicated by: Associate Editor Igor Tyukhov

Abstract

Most of PV modules designed to use bifacial cells are based on curved specular reflectors or on albedo reflectors to enhance the module output power. This paper describes PV modules assembled with bifacial cells and with a white aluminum reflector in order to enhance the solar radiation reaching the rear face of the solar cells. Two modules were fabricated by using p^+nn^+ bifacial cells and they were electrically characterized. The aluminum reflector with reflectance near to 90% for the wavelength range 350–1100 nm associated to the non-covered area between cell strings can enhance the output power of the modules in 29%. Modules with bifacial cells were installed in a stand-alone system in Porto Alegre, Brazil. After operation during 18 months, we observed that dust induced power degradation in the range of 1–4%, similar to that observed in standard modules. After cleaning, no power degradation was observed in the n-type bifacial cell modules. Temperature of bifacial cells estimated by infrared images was between 5 °C and 9 °C higher than that of standard modules. Bifacial cell modules presented the same behavior than standard modules when applied to stand-alone PV systems and achieved an average performance ratio of 0.79.

Keywords: Bifacial cells, PV modules; Stand-alone PV system

1. Introduction

Bifacial solar cells have been studied since 1960s years and their advantages stem from the possibility of converting the incoming solar radiation on both surfaces. Several solar cell structures were developed in order to use monocrystalline silicon wafers as starting material. Aberle (1999), Cuevas (2005) and Coello et al. (2006) presented reviews of the different approaches used to manufacture silicon bifacial solar cells. For instance, in p-type monocrystalline silicon, most efficient devices were developed by researchers of the Hitachi (Ohtsuka et al., 2000) by implementing a triode structure (with back contact n^+ and p^+ interleaved). Using float zone (FZ) silicon, the efficiencies of 21.3/19.8% were achieved for front/rear illumination. High efficiency simplified bifacial devices based on one pn junction and one back surface field region (BSF), i.e., n^+pp^+ structure, were presented by Yang et al. (2011) and Janβen et al. (2009). The former reported the results of industrial bifacial solar cells with large area fabricated with Cz-silicon and screen printed contacts. The best devices reached front and rear efficiencies of 16.6% and 12.8%, respectively (Yang et al., 2011). Janβen and coworkers (2009) also used Cz silicon and screen-printed contacts, but instead to implement a uniform p^+ region on the rear face, they deposit an Al metal grid to

* Corresponding author. Tel.: +55 51 3320 3682.
E-mail addresses: moehleck@pucrs.br (A. Moehlecke), filipesehn@gmail.com (F.S. Febras), izete@pucrs.br (I. Zanesco).
[1] She is a regular member of ISES, No. 0010999, since 08/1998.

0038-092X/$ - see front matter © 2013 Elsevier Ltd. All rights reserved.
http://dx.doi.org/10.1016/j.solener.2013.07.028

Nomenclature

I_{SC}	short-circuit current (A)
J_{SC}	short-circuit current density (mA/cm^2)
V_{OC}	open circuit voltage (V)
FF	fill factor
η	cell efficiency (%)
η_{Mod}	PV module efficiency (%)
I_{mpp}	current at maximum power point (A)
V_{mpp}	voltage at maximum power point (V)
P_{mpp}	maximum power (W)
PR	performance ratio
C_A	normalized array capacity
C_S	normalized storage capacity
LLP	loss of load probability

produce local BSF. The front efficiency of 17% and the rear efficiency of 10.3% were reported.

Phosphorus doped silicon has been studied as an alternative to boron doped Si because n-type wafers have higher tolerance to defects and impurities like iron (MacDonald and Geerligs, 2004) as well as solar cells did not present the light-induced degradation (LID) (Saitoh et al., 1999). For example, by using FZ n-type silicon, Guo and Cotter (2004) presented two kinds of laser-grooved bifacial solar cells, one with metal grid on both faces and other with interdigitated metal grids on the rear face. Efficiencies of 16.6/16.2% for the former and of 17/15.7% for the second device were reported when devices were illuminated by front and rear faces, respectively. Back-point contact solar cells were also developed in n-type FZ wafers and bifacial devices achieved efficiencies of 21.9/13.9% and 20.6/15.2% for front/rear illumination. Differences in efficiency were due to the metal area coverage of the rear face: 20% and 10%, respectively (Zhou et al., 1997). A new concept of interdigitated back contact, called "Zebra" technology, was presented recently and the authors proposed to use them in bifacial modules (Galbiati et al., 2013). To produce the "Zebra" cells, the fabrication process sequence did not need expensive lithographic steps and interdigitated back-contacts are implemented by screen-printing as well as Cz wafers were used. Efficiency of cells for back illumination was not presented, but the integration of the output power over one day showed an improvement of about 12% for the module with bifacial cells compared to that with monofacial ones, when the modules were installed over a ground with reflectance of around 70%, faced south (north hemisphere) and tilted of 30°.

Heterojunction with intrinsic thin layer (HIT) solar cell is another n-type bifacial device. It was developed by Sanyo and has been continuously studied and improved (Taguchi et al., 2000; Mishima et al., 2011; Tohoda et al., 2012; Dwivedi et al., 2013). Instead to use typical homojunctions obtained by diffusion or ion implantation, junction is produced by depositing thin-films of amorphous silicon. Efficiencies of 23% were obtained and researchers reported that the output power of the modules with bifacial cells can be enhanced by more than 10% over the single side module (Mishima et al., 2011). Another approach to fabricate bifacial cells was presented by Bruk et al. (2009) and Simashkevich et al. (2011). Solar cells were manufactured with two isotype junctions in a n-type wafer and front junction was obtained by depositing an indium tin oxide (ITO) layer. The back surface field region was produced by phosphorus diffusion (Bruk et al., 2009).

The standard p^+nn^+ structure with homogenous doped regions was developed in FZ and Cz-silicon solar cells, achieving efficiencies of 19.1/18.1% (front/rear illumination) and 17.7/15.2%, respectively, employing metal contacts defined by photolithography (Moehlecke et al., 1994, Cañizo et al., 2001). Buck et al. (2006) obtained efficiencies of 15.9/13.4% (front/rear illumination) in large area p^+nn^+ devices fabricated by using FZ silicon and with metal grid deposited by screen-printing. Recently, Böscke et al. (2013) reported results from large area p^+nn^+ solar cells, also with homogeneous p^+ and n^+ regions, but the details of the process were not presented. Cell achieved an efficiency of around 20% when it was illuminated by front face. Instead of presenting the efficiency of solar cells when illuminated by rear face, the authors commented that bifacial cells could improve the efficiency of a single side module of around 10%.

First photovoltaic modules proposed to use the dual face illumination in terrestrial applications were based on flat mirrors that directed sunlight to the rear face of the solar cells (Cuevas, 2005). Instead to use mirrors, albedo collecting modules were developed in 80ś by using bifacial cells and combinations of white-painted surfaces (Cuevas et al., 1982; Cuevas, 2005). In a work that deal with the estimation of radiation incident on bifacial modules, Krenzinger and Lorenzo (1986) reported that annual solar radiation incident on bifacial modules produced by the different orientated configurations of white painted reflector planes could be nearly 70% higher than that collected by conventional monofacial ones.

Moehlecke and Krenzinger (1991) proposed and analyzed two kinds of modules assembled with diffuse reflectors and bifacial cells. In those modules, the cells were laminated keeping a space between them in order to allow the solar radiation to reach the flat diffuse reflector. Then, the reflected radiation can strike on the rear face of bifacial cells. Module worked like the albedo-collecting one, but it is independent of the surroundings and the installation did not require a physical separation from roof or architectural elements of buildings. One of the modules proposed had an air gap between the plane of cells and white reflector and the other had the gap filled with a dielectric transparent material to enhance the irradiance on the back face of the solar cells by total internal reflection. Round solar cells equally spaced were used. Taking into account cost considerations to optimize the dimensions, the authors concluded that in optimal modules with air gap and dielectric filled gap reached about 25% and 40% more radiation on the cells than a conventional monofacial module with the same cell-area, respectively. Optimum thickness of the module with filled gap was 10% of that of the air gap module. For application of the PV modules in façades or as a building integrated element, colored reflectors were proposed (Moehlecke et al., 2001). By using a small experimental prototype, the performance of different colored reflectors was compared and it was concluded that yellow and orange reflector can be used with a reduction in performance lower than 7% when compared with white reflectors. Silveira et al. (2003) proposed to use strings of pseudo-square bifacial cells, as shown in Fig. 1, instead of the round cells of the first prototypes presented by Moehlecke and Krenzinger (1991). Dimensions of the module with white-painted reflector were optimized taking into account the radiation incident on the rear face of the bifacial cell strings as well the cost of assembling materials. Although the solar radiation reaching the rear face of solar cells rely on the space between strings and on the distance from cells to white reflector, cost evaluation showed that the thickness has to remain lower than 60 mm, if the space between strings is from 60% to 200% of the solar cell length. Best distance between strings encountered was 100 mm, that is the length of the pseudo-square cell considered. Therefore, 50% of module area was covered with solar cells. From simulation of the module during one year with bifacial cells with a rear efficiency of 85% of front efficiency, the authors reported that module produced 35% more energy than a standard one with the same cell area. Febras et al. (2009) assembled two prototypes with white reflector aiming to analyze the irradiance distribution on the rear face of the strings as well

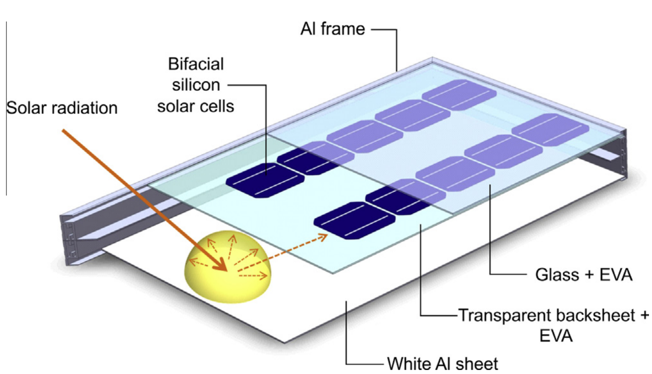

Fig. 1. PV module with bifacial cells and diffuse back reflector.

as to obtain the best orientation of solar cell strings, south-north or west-east, for modules 48° tilted to horizontal plane at Porto Alegre, Brazil (latitude = −30°). Monofacial cells were installed to measure the irradiance on the rear face of the bifacial cells in five regions of the prototypes. The best radiation collection was obtained by prototypes with south-north orientated strings. The module performance was limited by the lower radiation reaching the rear face of bifacial cells near the edge of the modules.

Modules with bifacial cells and white reflector were proposed to use as sun-shading element in façades or as a roof of carports, typical applications in the framework of BIPV (building integrated photovoltaics) (Hezel, 2003). Strings composed of square bifacial solar cells were laminated between two glass sheets and they were arranged keeping the distance of one cell-length between them. The white reflector was attached to the module as an external element. One of the prototypes presented four strings of 10 cells, 100 × 100 mm in size.

Uematsu et al. (2001, 2003) developed flat-plate static-concentrator modules with v-groove reflector instead of white painted reflectors. To manufacture the module, 32 bifacial cells (area of 24 mm × 80 mm) were soldered in eight strings with four cells each. Space between strings was 12 mm and the cells covered 67% of the module area. Flat module was 4 mm thick and had an area of 378 mm × 349 mm. The influence of the orientation of the strings was analyzed and the authors reported that about 90% of the annual irradiation in Tokyo can be collected by flat-plate static concentrator and the output power was 2% larger than that obtained from standard modules.

Experimental results from bifacial modules integrated with external diffuse and semimirror reflector were recently reported by Ooshaksaraei et al. (2013). Angle of reflector and separation between solar cells and reflector were addressed by using a solar simulator. A prototype was manufactured with four 5″ × 5″ monocrystalline bifacial silicon solar cells equally spaced covering 69% of the total area. Maximum power was obtained when the module + semimirror back reflector and module + diffuse reflector was tilted 30° and 10° with respect to the horizontal, respectively. In both cases, the optimized reflector-module separation was 115 mm.

The aim of this paper is to present the experimental evaluation of PV modules with p^+nn^+ bifacial solar cells and a white diffuse reflector. Bifacial solar cells were fabricated and characterized and two PV modules were manufactured following industrial standard assembling process. Modules were characterized after the manufacturing and after 18 months of operation in a PV stand-alone system installed in Porto Alegre, Brazil. Performance of PV modules with bifacial cells was compared to that of modules with standard monofacial cells installed in a similar stand-alone system. Moreover, the effect of dust deposition and the degradation of the modules were analyzed.

2. Fabrication and characterization of p^+nn^+ bifacial cells

The process to fabricate p^+nn^+ bifacial silicon solar cells was developed at NT-Solar/PUCRS and it is summarized in Fig. 2. The starting material was PV-FZ™ silicon, n-type, phosphorus doped, 1–15 Ω cm, ⟨1 0 0⟩ orientation and 300 μm thick. Texture etch was done in an alkaline solution based on KOH and isopropyl alcohol, the latter used to improve the uniformity of the random pyramid texture. Wafers were cleaned in RCA standard solutions (Kern, 1993) and a 100 nm thick SiO_2 layer was grown at 1000 °C in a quartz tube furnace. Photoresist was spin coated on one face and the non-covered oxide layer was etched away in a buffered HF solution. After RCA cleaning of the wafers, phosphorus diffusion using liquid $POCl_3$-based source was performed. Phosphorus silicate glass (PSG) and SiO_2 layer were removed in a HF bath and wafers were cleaned. Commercially available solution composed of boron and solvents (PBF20, Filmtronics, USA) was used to produce the p^+ region. Boron solution was deposited by spin-on and to evaporate the solvents, a baking at 200 °C was carried out. Boron was diffused at 1000 °C in a quartz tube furnace and boron silicate glass (BSG) was removed in a HF solution. The p^+ and n^+ regions presented an average sheet resistance of (25 ± 3) Ω/□ and (20 ± 1) Ω/□, respectively. Wafers were cleaned in a RCA solution and an antireflection coating (ARC) of TiO_2 (68 nm thick) was deposited on both faces by e-beam evaporation at high vacuum (pressure lower than 8.5×10^{-5} torr). The metal grids, with 38 fingers (100 μm wide) and 2 busbars were obtained by screen-printing and we used an Ag paste (PV156, DuPont, USA) on the n^+ face (rear) and an Ag/Al paste (PV202, DuPont, USA) on the p^+ face (front). Metal pastes were dry and co-fired in a belt furnace. Pseudo-square cells (80 mm × 80 mm) were obtained after the laser edge isolation process.

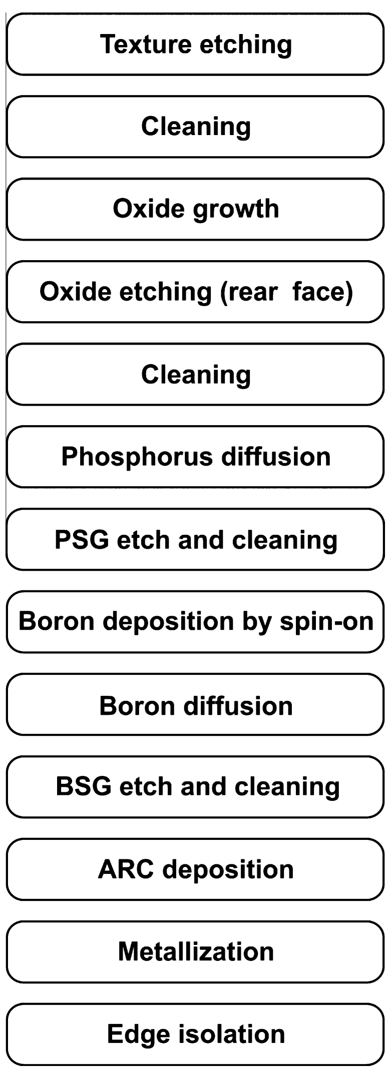

Fig. 2. Fabrication process sequence used to produce p^+nn^+ bifacial silicon solar cells.

Table 1
Average electrical characteristics of p^+nn^+ bifacial solar cells under standard conditions (100 mW/cm^2, AM1.5 G, 25 °C).

V_{OC} (mV)	J_{SC} (mA/cm^2)	FF	η (%)
ModBifa 01 (36 cells)			
Illumination by front face – p^+			
601.6 ± 1.8	32.5 ± 0.2	0.71 ± 0.01	13.8 ± 0.2
Illumination by rear face – n^+			
604.3 ± 2.4	29.5 ± 0.3	0.74 ± 0.01	13.2 ± 0.2
ModBifa 02 (36 cells)			
Illumination by front face – p^+			
602.1 ± 2.6	32.1 ± 0.4	0.71 ± 0.02	13.7 ± 0.2
Illumination by rear face – n^+			
605 ± 3	29.3 ± 0.6	0.74 ± 0.01	13.1 ± 0.2

All the devices were characterized under standard conditions (100 mW/cm^2, AM1.5G and 25 °C) in a solar simulator calibrated with silicon solar cells previously measured at CalLab-FhG-ISE (Fraunhofer-Institut für Solare Energiesysteme), Germany. Solar cells were classified in two sets taking into account the short-circuit current (I_{SC}). Table 1 presents the average characteristics of each set of bifacial cells used in PV modules and Fig. 3 shows the current density–voltage (J–V) characteristics of a typical solar cell. Efficiencies of around 14% were obtained without surface passivation based on silicon nitride or silicon dioxide. The low fill factors caused by the Ag/Al front metal grid limited the efficiency. Similar results were obtained for rear illumination mode due to the high bulk minority carrier lifetime in FZ wafers used. However, it is worth to mention that p^+nn^+ cells processed by using solar grade n-type Cz-Si achieved the efficiencies of 13.5% (Zanesco et al., 2012).

3. Fabrication of the modules

Two PV modules were fabricated with 36 bifacial cells in order to achieve the typical voltage of 12–14 V to charge

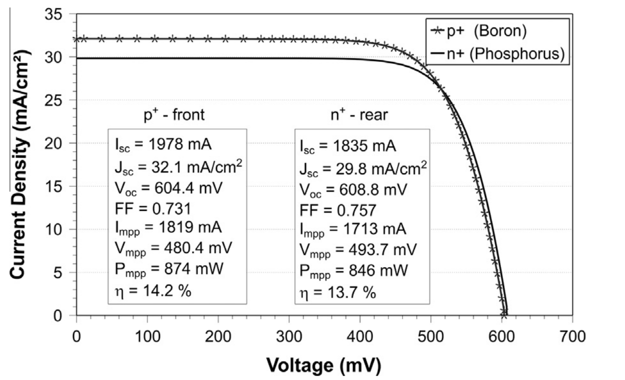

Fig. 3. Electric current density as a function of voltage (*J*–*V*) of a typical p^+nn^+ bifacial cell used to fabricate the PV modules.

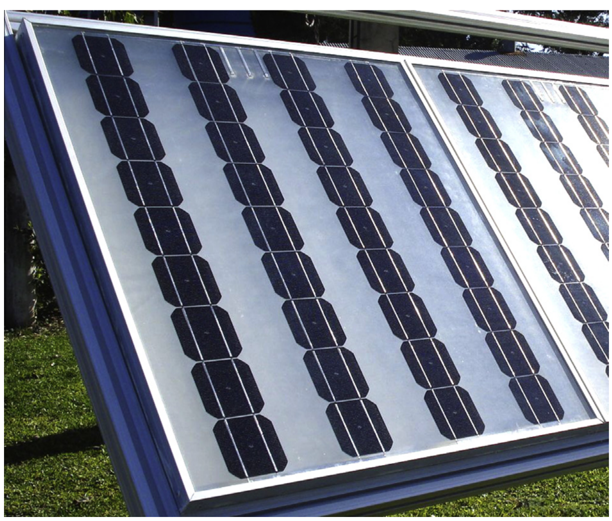

Fig. 4. PV module with bifacial cells and with a white diffuse reflector.

batteries in stand-alone systems. These modules were called ModBifa. Four strings of nine cells were used in order to allow the introduction of two by-pass diodes to protect two strings independently, preventing hot-spot heating. Each bifacial cell string was soldered by an automatic tabber-stringer equipment and lamination was performed by using high transparence tempered glass, fast cure EVA and transparent backsheet (Primer + Tedlar® + PET, 100 μm/25 μm/175 μm). The module had the following dimensions: 775 mm × 690 mm × 70 mm. The area of modules was of around 0.535 m². The distance between the strings was 80 mm (the length of one pseudo-square cell) according to the results of a previous work that dealt with the optimization of the dimensions of modules with diffuse reflectors (Silveira et al., 2003). As we commented in the introduction, Silveira et al. (2003) reported that the distance between strings must be of one cell length taking into account the performance and the cost of the module. This distance from string to string was also used by Hezel (2003) in the prototypes with white reflectors attached.

Two aluminum frames 35 mm thick developed to monofacial standard modules were attached by using screws and the PV804 silicone (supplied by Dow Corning®) was used to seal the module. Therefore, the thickness of the module was of around 70 mm and the distance between the glass and the aluminum reflector was 60 mm, according to the optimization performed by Silveira et al. (2003). Fig. 4 presents one of the modules fabricated with bifacial cells.

To obtain the white diffuse reflector, several commercially available white paintings were analyzed by measuring the hemispherical reflectance in the wavelength range from 350 nm to 1100 nm. The best white paint over aluminum sheet presented an average reflectance above 90% for the wavelength range 350–1100 nm. Samples of white-painted aluminum sheet covered with EVA and glass were exposed to ultraviolet radiation according to International Standard IEC 61345 (1998) by using an accelerated weathering chamber and other samples were exposed to outdoor conditions by 18 months and no reflectance degradation was observed (Febras, 2008).

4. Electrical characterization of the PV modules

4.1. After fabrication

PV modules were electrically characterized by measuring the current–voltage (*I*–*V*) curve under standard conditions by using a solar simulator Bergerlichtechnik PSS8, class AAA. Solar simulator was calibrated with a PV module previously calibrated in the European Solar Test Installation (ESTI), Joint Research Center-European Community, Italy. The electrical characteristics of encapsulated bifacial cells were measured with illumination by n^+ face (rear) and p^+ face (front). After to seal the set composed of glass, the frames and reflector and to attach the junction box, the *I*–*V* curve of the completed module was measured.

Fig. 5 presents the *I*–*V* characteristics of the encapsulated cells and of the two modules produced. When the encapsulated cells were illuminated by front face, short-circuit current of 2.0 A is slightly higher than that from the cells (see Fig. 3). The open circuit voltage (V_{OC}) of the modules corresponds to that from 36 cells in series. The fill factor (FF) is higher than that from the cells because the tabs reduce the electrical resistance of the 2 mm wide busbars with Ag–Al paste. When the module was illuminated by the rear face, i.e., by n^+n region of the bifacial solar cells, there was a high difference between short-circuit current of the solar cells and of the modules. Cells presented an I_{SC} from 1.80 A to 1.82 A and modules achieved only 1.50–1.53 A. All the cells were electrically characterized and for the ModBifa 01, the worst cell presented an I_{SC} of 1.78 A and for the ModBifa 02, the lowest I_{SC} was 1.75 A. The lower I_{SC} of the module for rear illumination is due to shadow produced by the aluminum frame over the edge cells in every string.

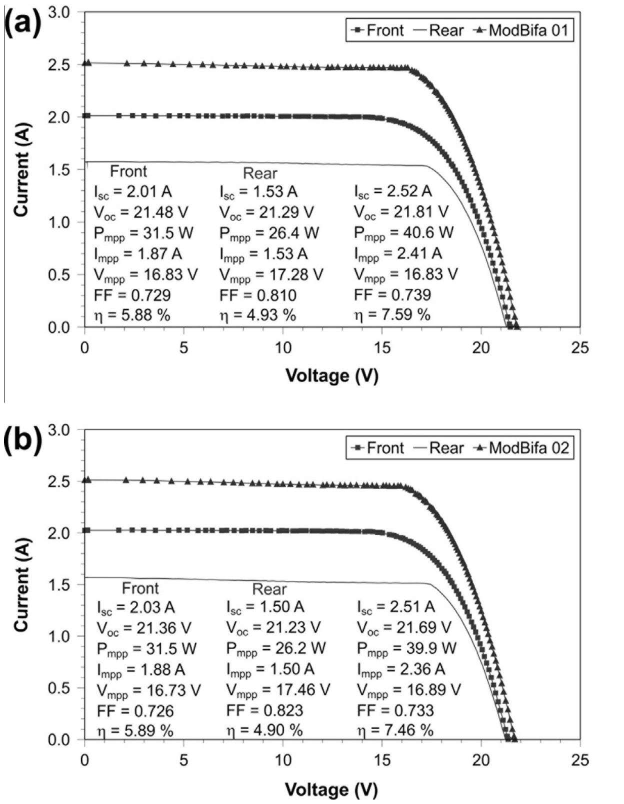

Fig. 5. Current density as a function of applied voltage, measured under standard conditions, for (a) ModBifa 01 and (b) ModBifa 02. Front and rear illuminated electric parameters were obtained before to attach the reflector.

As shown in Fig. 5, the white-painted reflector enhanced the short-circuit current of around 25% and the output power of the modules was increased from 31 W to 40 W (29% higher).

4.2. After exposure to radiation

Two stand-alone systems were installed: one with the modules ModBifa connected in parallel and other with two standard modules with n^+pp^+ monofacial cells, also connected in parallel. Standard modules were also fabricated at NT-Solar/PUCRS in a pilot plant that produced 12,000 n^+pp^+ Cz–Si solar cells and 220 modules (Moehlecke and Zanesco, 2012). Since the dimensions of the bifacial and monofacial cells were the same, cell area was equal for both systems. PV modules were installed in a surface tilted 48°, faced to north, optimized for stand-alone systems installed in Porto Alegre, Brazil (Zanesco et al., 2004). Total irradiance on the modules was measured with an Eppley PSP pyranometer. Systems were monitored by 18 months, from October, 2010 to March, 2012. Fig. 6 presents the monthly total solar radiation during the period that the modules were exposed. Total irradiation in the period was of 1.9 MW h/m^2 (6.7×10^9 J/m^2).

Electrical characteristics of the modules were measured after the exposure, before and after the cleaning of the

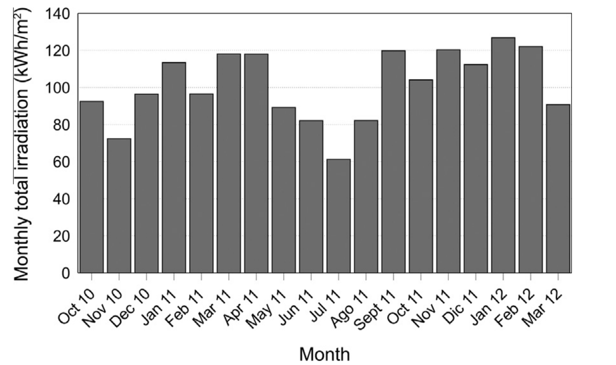

Fig. 6. Monthly total irradiation concerning the period that the modules were operating in PV stand-alone systems. Total irradiation during the 18 months was of 1.9 MW h/m^2 (6.7×10^9 J/m^2).

PV modules. Table 2 summarizes the results obtained from standard modules and modules with bifacial cells.

Before the cleaning, visual inspection of the modules indicated dust accumulation, mainly on the bottom edge of the modules. The power of modules with bifacial cells degraded of about 1% and 4% for the modules ModBifa 01 and 02, respectively. In the same way, the power of standard modules 111 and 129 fell of 1% and 5.5%, respectively. Main parameter that decayed was the short-circuit current. Therefore, the power degradation due the dust deposition in modules with bifacial cells and white reflector is similar to that observed in standard modules. The dust deposition depends on several conditions like the site, the weather, the module tilt angle, the kind of glass surface, etc., but similar values of power losses were presented by several authors (Haeberlin and Graf, 1998; Hammond et al., 1997; Casanova et al., 2012). Haeberlin and Graf (1998) monitored during four years a 60 kW$_p$ system installed in Switzerland and they concluded that dust accumulation over the PV modules can reduce the power from 8% to 10% during the summer months due to pollution. In Arizona, USA, Hammond and coworkers (1997) concluded that I_{SC} decreased by 3% due to the soiling during the first nine months after installation and periodic cleaning produced by rain recovered the 99.5% of initial output. Casanova et al. (2012) observed that mean daily irradiation losses in a year caused by dust deposited on the surface of a silicon-based PV module were of around 4% for modules installed in Malaga, Spain (latitude = 36.7°) on a surface tilted 30°. These results are similar to I_{SC} degradation observed in Porto Alegre and presented in Table 2.

After cleaning, we observed that most electrical parameters of the modules with bifacial n-type cells was increased. The enhancement is in the range of uncertainty of measuring I–V characteristics with solar simulator and we can conclude that cells, encapsulating material and white diffuse reflector do not degrade after exposure to outdoor conditions after 18 months. On the other hand, standard modules presented lower I_{SC} and P_{mpp}, of around 3.2% and 2.2% lower, respectively. The 1.5% reduction in maximum power per year is higher than that reported in

Table 2
Comparison of electrical characteristics measured after PV module manufacturing, after exposure to outdoor conditions by 18 months before and after cleaning the modules. Δ_1 is the difference between initial electrical parameters and after outdoor exposure and Δ_2 is the difference between initial value and after cleaning the glass sheet.

	ModBifa 01					ModBifa 02				
	After fabrication	After exposure	Δ_1 (%)	Cleaned	Δ_2 (%)	After fabrication	After exposure	Δ_1 (%)	Cleaned	Δ_2 (%)
V_{OC} (V)	21.8	21.4	−1.8	21.5	−1.4	21.7	21.6	−0.5	21.7	0
I_{SC} (A)	2.52	2.36	−6.4	2.53	+1.1	2.51	2.41	−4.0	2.58	+2.8
FF	0.739	0.769	+4.0	0.748	+1.2	0.733	0.758	+3.4	0.736	+0.4
P_{mpp} (W)	40.6	38.9	−4.2	40.8	+0.5	39.9	39.5	−1.0	41.1	+3.0
η (%)	7.59	7.28	−4.1	7.63	+0.5	7.46	7.38	−1.1	7.68	+2.9
	Standard module 111					Standard module 129				
V_{OC} (V)	20.6	20.9	+1.5	20.6	0	21.0	20.9	−0.5	20.9	−0.5
I_{SC} (A)	2.10	1.99	−5.2	2.03	−3.3	2.16	1.99	−7.9	2.09	−3.2
FF	0.767	0.791	+3.1	0.778	+1.4	0.766	0.790	+3.1	0.778	+1.6
P_{mpp} (W)	33.3	32.9	−1.2	32.6	−2.1	34.7	32.9	−5.2	34.0	−2.0
η (%)	11.9	11.8	−0.8	11.7	−1.7	12.4	11.8	−4.8	12.2	−1.6

other works that deals with the degradation of crystalline silicon modules (Sánchez-Friera et al., 2011; Jordan and Kurtz, 2013; Munoz et al., 2011), when 0.5–1.1% was observed. However, Munoz et al. (2011) commented that the maximum power of crystalline silicon PV modules can be reduced from 1% to 4% during the initial days of operation due to initial power stabilization. It is worth to comment that bifacial cells were produced with n-type PV-FZ silicon and monofacial ones with p-type (boron doped) solar grade Cz–silicon. The former does not have any physical mechanism for light-induced degradation whereas Cz can present degradation (Saitoh et al., 1999).

4.3. Comparison of the bifacial and monofacial solar cell temperatures

Operation temperature of bifacial cells was estimated by using an infrared camera FLIR model I60. Fig. 7 presents the infrared image obtained with a cloudless sky in a spring day. During the data acquisition, ambient temperature was of 28 °C and irradiance in the plane of the modules was 700 W/m^2. Temperature of bifacial cells in the modules was 9 °C higher than that in standard modules. During the 18 months, infrared images obtained in cloudless days indicated that the temperature of bifacial cells was from 5 °C to 9 °C higher than the temperature of the cells in standard modules. This result was produced due to the higher irradiation on bifacial solar cells and because heat transfer in the rear face of the cells was due to the convection in a closed space formed by glass, aluminum frames and reflector.

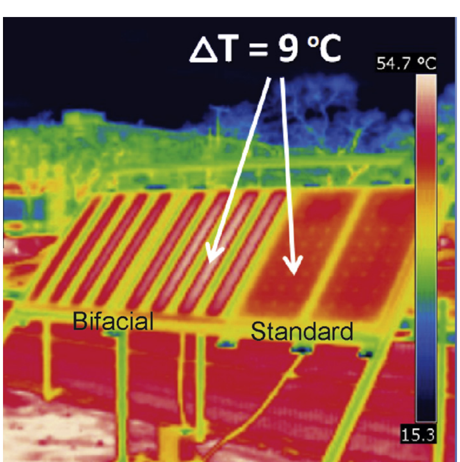

Fig. 7. Thermographic image of modules obtained in a cloudless day in spring.

5. Application to the stand-alone systems

Two stand-alone systems were implemented: one with two ModBifa modules in parallel, that we called BIFACIAL system and another with two standard modules with n$^+$pp$^+$ monofacial cells, called STANDARD, connected also in parallel. Power of the BIFACIAL and STANDARD system was of 80.5 W$_p$ and 68.1 W$_p$, respectively. BIFACIAL system was designed to achieve a loss of load probability near 1×10^{-2} in Porto Alegre, Brazil, taking into account the work developed by Zanesco et al. (2004) that deals with the sizing of PV stand-alone systems in Brazil. Both systems had two lead-acid batteries designed for PV, totalizing a capacity of 300 Ah, one charge regulator, four fluorescent lamps of 20 W and one small inverter per lamp. The normalized PV generator size × normalized storage capacity (pair $C_A \times C_S$) was 1.21×7 for BIFACIAL system and 1.09×7 for STANDARD one. Lamps operated every day after 7 pm, resulting a load demand of 0.3 kW h/day (1.08×10^6 J/day).

In order to characterize the systems, a data acquisition system was installed based on Agilent 34970 and 34901A equipments. The following parameters were measured each 10 min: (1) PV array voltage; (2) PV array current by measuring the voltage in a shunt (1 mΩ ± 1%); (3) electric current in the charge (also by using a shunt); (4) battery voltage; (5) total irradiance.

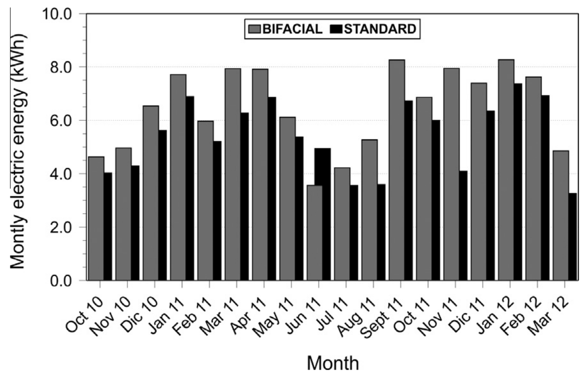

Fig. 8. Monthly electric energy produced and stored by PV stand-alone systems.

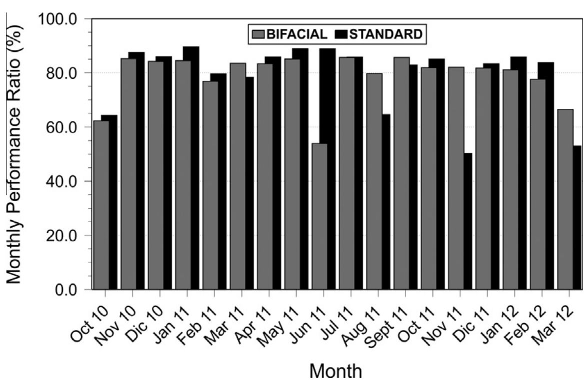

Fig. 9. Monthly performance ratio of both stand-alone systems.

Figs. 8 and 9 present the monthly electrical energy produced and the monthly performance ratio (PR) of both systems. The PR is the ratio of the final PV system yield to the so-called reference yield (Reich et al., 2012). In other words, the ratio between the actual energy output to the energy output that considered the solar radiation on the plane of the module and the efficiency at standard conditions. To calculate the latter, an efficiency of 7.5% under standard conditions and an area of 1.073 m^2 were considered for BIFACIAL system. For STANDARD system, the efficiency was of 12.1% and the area was of 0.563 m^2. Monofacial and bifacial cells presented similar efficiencies and the difference in module efficiency was due to the higher area of ModBifa modules than standard ones.

Higher operating temperature than that used in standard conditions, optical losses due to the glass reflection or dust deposition, conduction losses in wiring and charge regulator, inverter efficiency, etc. are currently factors that reduces the PR. The average PR for both systems installed was of 79%, a typical value of grid connected systems (Reich et al., 2012) and higher than the value of 60% mentioned as good for well-installed stand-alone systems (Díaz et al., 2007; Mayer and Heidenreich, 2003). Both systems presented PR near 80% in 15 months as shown in Fig. 9. Lower values of PR, of around 52–54%, were observed in three months, when the systems presented fails due to charge regulator and inverters. For instance, in June 11, stand-alone system with bifacial modules presented a fail in the charge regulator and electric energy was not storaged in the batteries during several days, reducing the monthly electric energy and PR.

6. Conclusions

Two PV modules were fabricated by using p^+nn^+ bifacial solar cells and a white-painted aluminum sheet with reflectance of 90%. By keeping a space of one-cell length between each cell string, we observed that the aluminum back reflector enhanced the output power of the modules of around 29%.

Modules fabricated were exposed to solar irradiation in Porto Alegre, Brazil, by 18 months in a surface tilted of 48°. We observed that dust reduced the power of the modules in the range of 1–4%. These results were similar to that encountered in the standard modules and that published by other authors for modules installed at several sites around the world. After cleaning the modules, we observed that modules with bifacial n-type solar cells did not present any performance degradation.

The operating temperature of the bifacial cells was only 5–9 °C higher than that of standard modules.

The same average performance ratio of 0.79 was calculated for systems with modules based on bifacial cells and monofacial cells. The system operation was similar for both kinds of modules analyzed.

Concerning the assembly of the PV modules with bifacial p^+nn^+ cells and white reflector, we concluded that the same technique used to fabricate standard modules can be applied. The use of larger area glass, higher amount of aluminum (frame and reflector sheet) and silicone sealing than those used in the standard modules besides the use of white paint enhance the fabrication cost of the modules. However, the cost estimation will depend on the cost and the efficiency of bifacial cells produced in large scale.

Acknowledgments

The financial supports by the Brazilian financing agency FINEP (Financiadora de Estudos e Projetos), CEEE (Companhia Estadual de Energia Elétrica) and CNPq (Conselho Nacional de Desenvolvimento Científico e Tecnológico) are gratefully acknowledged. The authors would like to thank the staff of NT-Solar/PUCRS engaged to process silicon solar cells.

References

Aberle, A., 1999. Crystalline Silicon Solar Cells: Advanced Surface Passivation and Analysis. University of New South Wales, Sidney.

Böscke, T.S., Kania, D., Helbig, A., Schöllhorn, C., Dupke, M., Sadler, P., Braun, M., Roth, T., Stichtenoth, D., Wütherich, T., Jesswein, R., Fiedler, D., Carl, R., Lossen, J., Grohe, A., Krokoszinski, H.J., 2013. Bifacial n-type cells with >20% front-side efficiency for industrial production. IEEE Journal of Photovoltaics 3 (1), 674–677.

Bruk, L., Fedorov, V., Sherban, D., Simashkevich, A., Usatii, I., Bobeico, E., Morvillo, P., 2009. Isotype bifacial silicon solar cells obtained by ITO spray pyrolysis. Materials Science and Engineering B 159–160, 282–285.

Buck, I., Kopecek, R., Libal, J., Herguth, A., Peter, K., Rover, I., Wambach, K., Geerligs, B., 2006. Industrial screen printed n-type silicon solar cells with front boron emitter and efficiencies exceeding 17%. In: Proceedings of the 21st European Photovoltaic Solar Energy Conference, pp. 1264–1267.

Cañizo, C., Moehlecke, A., Zanesco, I., Tobías, I., Luque, A., 2001. Analysis of a technology for CZ bifacial solar cells. IEEE Transactions on Electron Devices 48 (10), 2337–2341.

Casanova, J.Z., Piliougine, M., Carretero, J., Bernaola-Galván, P., Carpena, P., Mora-López, L., Sidrach-de-Cardona, M., 2012. Losses produced by soiling in the incoming radiation to photovoltaic modules. Progress in Photovoltaics: Research and Applications. Published online in Wiley Online Library (wileyonlinelibrary.com). doi: http://dx.doi.org/10.1002/pip.1258.

Coello, J., Cañizo, C, Luque, A., 2006. Review on bifacial solar cell structures for industrialization. In: Proceedings of the 21st European Photovoltaic Solar Energy Conference, pp. 1358–1361.

Cuevas, A., 2005. The early history of bifacial solar cells. In: Proceedings of the 20th European Photovoltaic Solar Energy Conference, pp. 801–805.

Cuevas, A., Luque, A., Eguren, J., del Alamo, J., 1982. 50% more output power from an albedo-collecting flat panel using bifacial solar cells. Solar Energy 19, 419–420.

Díaz, P., Egido, M.A., Nieuwenhout, F., 2007. Dependability analysis of stand-alone photovoltaic systems. Progress in Photovoltaics: Research and Applications 15, 245–264.

Dwivedi, N., Kumar, S., Bisht, A., Patel, K., Sudhakar, S., 2013. Simulation approach for optimization of device structure and thickness of HIT solar cells to achieve ~27% efficiency. Solar Energy 88, 31–41.

Febras, F.S., 2008. Development of Static Concentrator Modules with Diffuse Reflector. M.Sc. Thesis, Pontifical University of Rio Grande do Sul, Brazil (in Portuguese).

Febras, F.S., Moehlecke, A., Zanesco, I., 2009. Experimental study of static concentrator modules with diffuse reflector. In: Proceedings of the 24th European Photovoltaic Solar Energy Conference, pp. 807–810.

Galbiati, G., Mihailetchi, D., Roescu, R., Halm, A., Koduvelikulathu, L.J., Kopecek, R., Peter, K., Libal, J., 2013. Large-area back-contact back-junction solar cell with efficiency exceeding 21%. IEEE Journal of Photovoltaics 3 (1), 560–565.

Guo, J.H., Cotter, J.E., 2004. Laser-grooved backside contact solar cells with 680-mV open-circuit voltage. IEEE Transactions on Electron Devices 51 (12), 2186–2192.

Haeberlin, H., Graf, J.D., 1998. Gradual reduction of PV generator yield due to pollution. In: Proceedings of the 2nd World Conference and Exhibition on Photovoltaic Solar Energy Conversion, pp. 2764–2767.

Hammond, R., Srinivasan, D., Harris, A., Whitfield, K., Wohlgemuth, J., 1997. Effects of soiling on PV module and radiometer performance. In: Proceedings of the 26th IEEE PVSC, pp. 1121–1124.

Hezel, R., 2003. Novel applications of bifacial solar cells. Progress in Photovoltaics: Research and Applications 11, 549–556.

International Standard IEC 61345. UV test for photovoltaic (PV) modules, 1998.

Janβen, L., Windgassen, H., Bätzner, D.L., Bitnar, B., Neuhaus, H., 2009. Silicon nitride passivated bifacial Cz–silicon solar cells. Solar Energy Materials and Solar Cells 93, 1435–1439.

Jordan, D.J., Kurtz, S.R., 2013. Photovoltaic degradation rates—an analytical review. Progress in Photovoltaics: Research and Applications 21, 21–29.

Kern, W., 1993. Handbook of Semiconductor Wafer Cleaning Technology. Noyes Publications, New Jersey, USA, p. 623.

Krenzinger, A., Lorenzo, E., 1986. Estimation of radiation incident on bifacial Albedo-collecting panels. International Journal of Solar Energy 4 (5), 297–319.

Macdonald, D., Geerligs, L.J., 2004. Recombination activity of interstitial iron and other transition metal point defects in p- and n-type crystalline silicon. Applied Physics Letters 85 (18), 4061–4063.

Mayer, D., Heidenreich, D., 2003. Performance analysis of stand-alone PV Systems from a rational use of energy point of view. In: Proceedings of the Third World Conference on Photovoltaic Energy Conversion. <http://www.iea-pvps-task2.org/public/index.htm>.

Mishima, T., Taguchi, M., Sakata, H., Maruyama, E., 2011. Development status of high-efficiency HIT solar cells. Solar Energy Materials and Solar Cells 95, 18–21.

Moehlecke, A., Krenzinger, A., 1991. Modules assembled with diffuse reflectors for photovoltaic bifacial cells. In: Proceedings of the 10th European Photovoltaic Solar Energy Conference, pp. 967–970.

Moehlecke, A., Zanesco, I., 2012. Development of silicon solar cells and photovoltaic modules in Brazil: analysis of a pilot production. Materials Research 15 (4), 581–588.

Moehlecke, A., Zanesco, I., Luque, A., 1994. Practical high efficiency bifacial solar cells. In: Conference Record of the IEEE First World Conference on Photovoltaic Energy Conversion, pp. 1663–1666.

Moehlecke, A., Zanesco, I., Pan, A.C., Severo, T.C., Mallmann, A.P., 2001. Photovoltaic module with coloured diffuse reflectors. In: Proceedings of the 17th European Photovoltaic Solar Energy Conference, pp. 785–787.

Munoz, M.A., Chenlo, F., Alonso-García, M.C., 2011. Influence of initial power stabilization over crystalline-Si photovoltaic modules maximum power. Progress in Photovoltaics: Research and Applications 19, 417–422.

Ohtsuka, H., Sakamoto, M., Tsutsui, K., Yazawa, Y., 2000. Bifacial silicon solar cells with 21.3% front efficiency and 19.8% rear efficiency. Progress in Photovoltaics: Research and Applications 8 (4), 385–390.

Ooshaksaraei, P., Sopian, K., Zulkifli, R., Alghoul, M.A., Zaidi, S.H., 2013. Characterization of a bifacial photovoltaic panel integrated with external diffuse and semimirror type reflectors. International Journal of Photoenergy 2013, 7. Article ID 465837. doi: http://dx.doi.org/10.1155/2013/465837.

Reich, N.H., Mueller, B., Armbruster, A., Sark, W.G.J.H.M., Kiefer, K., Reise, C., 2012. Performance ratio revisited: is PR >90% realistic? Progress in Photovoltaics: Research and Applications 20, 717–726.

Saitoh, T., Hashigami, H., Rein, S., Glunz, S., 1999. Overview of light degradation research on crystalline silicon solar cells. Progress in Photovoltaics: Research and Applications 7, 426–436.

Sánchez-Friera, P., Piliougine, M., Peláez, J., Carretero, J., Sidrach de Cardona, M., 2011. Analysis of degradation mechanisms of crystalline silicon PV modules after 12 years of operation in Southern Europe. Progress in Photovoltaics: Research and Applications 19, 658–666.

Silveira, H., Zanesco, I., Moehlecke, A., 2003. Optimization of the modified static plain concentrator module. In: Proceedings of the 5th Latin-American Congress: Electricity Generation and Transmission, pp. 1–10.

Simashkevich, A.V., Sherban, D.A., Bruk, L.I., Kharya, E.E., Usatii, I.V., 2011. Efficient ITO-*n*Si solar cells with a textured silicon surface. Surface Engineering and Applied Electrochemistry 47 (3), 266–271.

Taguchi, M., Kawamoto, K., Tsuge, S., Baba, T., Sakata, H., Morizane, M., Uchihashi, K., Nakamura, N., Kiyama, S., Oota, O., 2000. HITTM cells – high efficiency crystalline Si cells with novel structure. Progress in Photovoltaics: Research and Applications 8, 503–513.

Tohoda, S., Fujishima, D., Yano, A., Ogane, A., Matsuyama, K., Nakamura, Y., Tokuoka, N., Kanno, H., Kinoshita, T., Sakata, H., Taguchi, M., Maruyamaet, E., 2012. Future directions for higher-efficiency HIT solar cells using a thin silicon wafer. Journal of Non-Crystalline Solids 358, 2219–2222.

Uematsu, T., Yazawa, Y., Joge, T., Kokunai, S., 2001. Fabrication and characterization of a flat-plate static-concentrator photovoltaic module. Solar Energy Materials and Solar Cells 67, 425–434.

Uematsu, T., Tsutsui, K., Yazawa, Y., Warabisako, T., Araki, I., Eguchi, Y., Joge, T., 2003. Development of bifacial PV cells for new applications of flat-plate modules. Solar Energy Materials and Solar Cells 75, 557–566.

Yang, L., Ye, Q.H., Ebong, A., Song, W.T., Zhang, G.J., Wang, J.X., Ma, Y., 2011. High efficiency screen printed bifacial solar cells on monocrystalline Cz silicon. Progress in Photovoltaics: Research and Applications 19, 275–279.

Zanesco, I., Moehlecke, A., Medeiros, G.S., Mallmann, A.P., Alcantara, S.P., 2004. Analytic method for sizing stand-alone systems in Brazil. In: Proceedings of the 19th European Photovoltaic Solar Energy Conference and Exhibition, pp. 2375–2378.

Zanesco, I., Moehlecke, A., Pinto, J.L., Ly, M., 2012. Development and comparison of small and large area boron doped solar cells in n-type and p-type Cz–Si. In: Proceedings of the 38th IEEE PVSC, pp. 2284–2288.

Zhou, C.Z., Verlinden, P.J., Crane, R.A., Swanson, R.M., Sinton, R.A., 1997. 21.9% Efficient silicon bifacial solar cells. In: Conference Record of the Twenty-Sixth IEEE Photovoltaic Specialists Conference, pp. 287–290.